Analysis of Microbolometer Characteristics for Antenna-Coupled Terahertz Detectors

Analysis of Microbolometer Characteristics for Antenna-Coupled Terahertz Detectors†

Ajay Tiwari[1], Hiroaki Satoh[1], Makoto Aoki[2], Masanori Takeda[2], Norihisa Hiromoto[2] and Hiroshi Inokawa[1,*]

[1]Research Institute of Electronics, Shizuoka University, 3-5-1 Johoku, Naka-ku, Hamamatsu 432-8011, Japan
[2]Graduate School of Science and Technology, Shizuoka University, 3-5-1 Johoku, Naka-ku, Hamamatsu 432-8011, Japan

*Corresponding author: Fax: +81 53 4781651; Tel: +81 53 4781308, E-mail: inokawa06@rie.shizuoka.ac.jp

Assuming the use in antenna-coupled bolometers to detect terahertz wave, an integrated heater and thermistor was fabricated with titanium on a silicon substrate and its responsivity was investigated at room temperature. To establish the correlation of microbolometer's responsivity on the properties of its thermistor and heater, an electro-thermal simulation was carried out for the resistance increase with current in thermally isolated heater and resultant increase of temperature. The behaviour of the heater resistance could be reproduced by the simulation successfully. The experimental responsivity shows opposite behaviour from the expected trend. This discrepancy was also explained by simulation and it was concluded that microbolometer with longer heater showed smaller responsivity due to the slower response for the measurement frequency.

Key Words: Far-infrared, Terahertz, Microbolometer, Photolithography, Electro-thermal simulation.

INTRODUCTION

Detectors for far-infrared (FIR) to terahertz (THz) waves are broadly classified into photon detectors and thermal detectors, both of them have generated a great deal of research interest over the last two decades[1,2]. Photon detectors are fast, more sensitive and commercialized for military and space science applications but require cooling systems to reduce the dark current. On the other hand thermal detectors, represented by a microbolometer, have ability to work at room temperature. Moreover, uncooled FIR-THz detectors are low-cost and more reliable and have found many applications in areas such as surveillance, firefighting, night vision, military, *etc*.[1]. However, uncooled bolometers have disadvantages, such as low detectivity due to thermal noise, response time, self-heating under constant bias[3] and susceptibility of the sensor material to the fabrication process[4].

An ordinary microbolometer consists of absorber that receives electromagnetic radiation and temperature sensitive resistor (thermistor). However, for longer wavelength, *e.g.*, in the tetrahertz region, the absorber becomes too large to be structurally supported and thermally isolated and then an antenna-coupled bolometer becomes more viable, in which the radiation is received by an antenna and converted to heat by a load resistor (heater). Historically, such microbolometer was made only with a thermistor that could be used commonly as a heater, but now the thermistor and heater are made separately to optimize the sensitivity[5].

Performance of such a microbolometer is mainly determined by (i) temperature coefficient of resistance (TCR) of the thermistor (ii) thermal isolation in the integrated structure of the heater and thermistor. Since the temperature distribution in the heater is disturbed by the presence of the thermistor, proper modeling is essential for evaluating and improving the characteristics of microbolometers[6]. This paper reports the fabrication and electro-thermal simulation of the integrated heater and thermistor for antenna-coupled microbolometers.

Fabrication process: The process steps in the fabrication of microbolometer are as follows. The thermistor on thermally oxidized (TO) Si substrate was formed by patterning of RF sputtered Ti thin film using photolithography as illustrated in Fig. 1(a). The interlayer SiO_2 was deposited by electron cyclotron resonance (ECR) sputtering. The contact hole in ECR sputtered SiO_2 was created by CHF_3 reactive-ion etching (RIE). After that, heater was fabricated by patterning of the sputtered Ti thin film as shown in Fig. 1(b). The deep-cavity for thermal isolation was formed by CHF_3 RIE and SF_6 plasma etching with sacrificial Al mask as shown in Fig. 1(c). The fabrication steps shown from Fig. 1(a-c) correspond to YY' cross-section (Fig. 2).
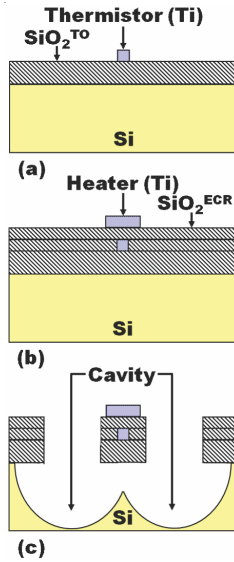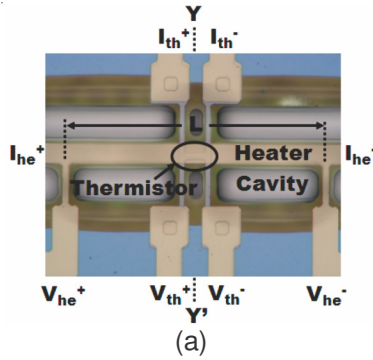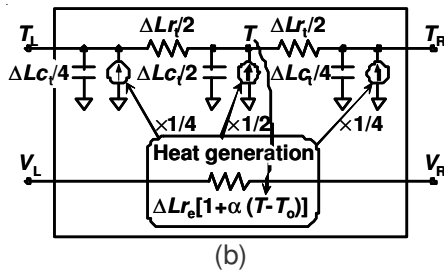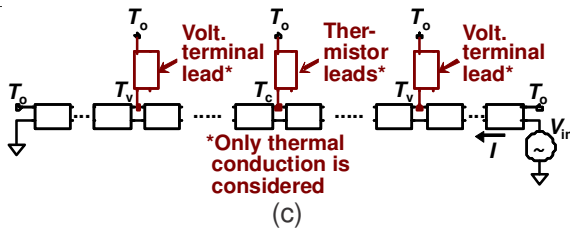
Fig. 1. Ti microbolometer fabrication steps along YY' cross-section. (a) Thermistor pattern, (b) heater pattern on top of ECR SiO$_2$ interlayer deposited on thermistor, and (c) suspended microbolometer structure above the cavity in Si substrate

Fig. 2. Fabricated device and its electro-thermal circuit for simulation. (a) Optical micrograph of the top view of the Ti microbolometer, (b) unit circuit and (c) entire circuit. Here I_{th}^+, I_{th}^- and V_{th}^+, V_{th}^- are current and voltage terminals respectively for thermistor, whereas I_{he}^+, I_{he}^- and V_{he}^+, V_{he}^- are similar terminals for heater

Electro-thermal simulation: To establish the correlation of the observed Ti microbolometer's responsivity, electro-thermal circuit simulation was carried out using SPICE circuit simulator. An optical micrograph of the top view of the fabricated microbolometer with their electrical connections is displayed in Fig. 2(a). The unit circuit representing heater/thermistor line with length (ΔL), thermal resistance (r_t), thermal capacitance (c_t), electrical resistance (r_e) and its temperature coefficient (α) is shown in Fig. 2(b) and the entire circuit including the heat loss through the thermistor and heater voltage-terminal leads is depicted in Fig. 2(c). Transient analysis was performed with sinusoidal input to V_{in} using SPICE circuit simulator and the temperature amplitude at T_c was converted to the thermistor output.

RESULTS AND DISCUSSION

After the device fabrication, the basic parameters were measured/calculated and listed in Table-1. Thickness of the heater/thermistor was measured by stylus profilometer and width and lengths were designed values. Resistance and temperature coefficient of resistance (TCR) were obtained by DC IV measurement at 240-300 K and the values for 300 K are listed.

TABLE-1
DEVICE PARAMETERS AND THEIR PROPERTIES

Parameters	Heater	Thermistor
Thickness (nm)	118	47
Width (µm)	15	5
Length (µm)	200, 400, 600, 800	20
Resistance	8.46×10^5 Ω/m	44.0 Ω
Temp. coef. (K^{-1})	2.14×10^{-3}	2.48×10^{-3}
SiO$_2^{TO}$ thickness (nm)	424	
SiO$_2^{ECR}$ thickness (nm)	89	
Cavity depth (µm)	41	

Thermal resistance of the heater line was evaluated based on the phenomenon that the electrical resistance of the heater increases with increasing DC current. The increase of the normalized resistance as function of square of the current is shown in Fig. 3. The normalized resistance linearly increases with the square of the current. The amount of the resistance change increases with heater length. For an isolated wire, the resistance change was observed and discussed analytically by Zhang et al.[7]. We have extended the analysis by our electro-thermal circuit simulation to incorporate heat loss caused by the leads of thermistor and the heater voltage terminal. It is clear from Fig. 3, the experimental data (symbols) fit very well with the simulated results (solid line) for each length. Fitting parameters for the simulation are thermal resistance per unit length of the heater (r_t), thermal capacitance (c_t), electrical resistance per unit length (r_e) and temperature coefficient of resistance (α), which are 1.97×10^{10} K/(Wm), 4.85×10^{-5} J/Km, 8.46×10^{-5} Ω/m and 2.14×10^{-3}, respectively. The r_t lies within 10 % of 1.79×10^{10} K/(Wm) calculated from the reported values of thermal conductances 1.32 W/(mK)[8] for SiO$_2$ and 21.9 W/(mK)[9] for Ti[9]. The simulated value of thermal capacitance is approximately 3 times higher than the values calculated for the Ti/SiO$_2^{ECR}$/SiO$_2^{TO}$ from the literature.

Furthermore, the electro-thermal circuit simulation was also used to calculate temperature distribution in each heater. The temperature profile for the input power of 10 µW is plotted
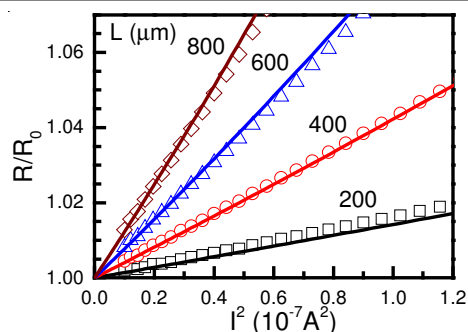
Fig. 3. Normalized resistance of the Ti microbolometers as a function of square of the applied current for each heater with different length. The symbols show experimental data, whereas solid lines show those by the simulation

against position in Fig. 4. At the both ends of the heater, the temperature is 300 K and increases slowly towards the center position. However, at the center there is sudden drop in the temperature, which is due to the heat loss through the thermistor leads. There are also deflection points near the ends of the heater caused by the heat loss by the voltage terminal leads of the heater.
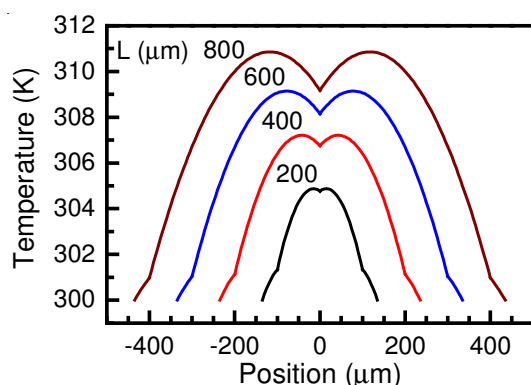
Fig. 4. Temperature distribution along the heater length predicted by electro-thermal circuit simulation

The responsivity of the fabricated microbolometers is measured by applying AC electrical power up to 50 µW at 10 Hz. Thermistor output was detected by lock-in-amplifier under the bias current of 0.5 mA. Thermistor output voltage with respect to the heater input power is shown in Fig. 5. The responsivity has a maximum value 14.6 V/W for heater length L of 200 µm and systematically decreases as the L increases.
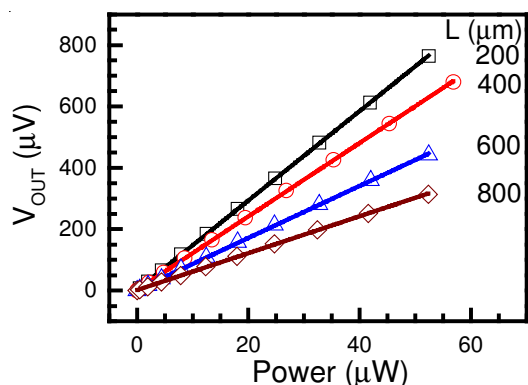
Fig. 5. Thermistor output voltage *versus* heater input power at 10 Hz for different heater lengths

The experimentally observed responsivity shows opposite trend from the expected behaviour, *i.e.* longer bolometers should have higher responsivity due to better thermal isolation. This discrepancy could be explained by simulation as illustrated in Fig. 6. At low frequencies, the responsivity tends toward the saturation and the simulation result behaves as expected. At high frequencies, the simulated trend shifts toward the experimental results. It can be concluded that the microbolometer with longer heater showed smaller responsivity due to the slower response for the measurement frequency.
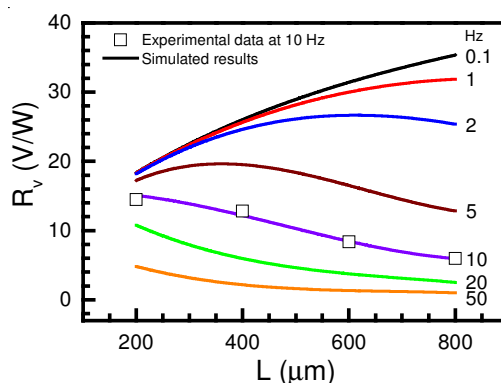
Fig. 6. The experimental and simulated responsivity of Ti microbolometer as function of heater length. The symbols show the experimental result, while solid lines show simulated results at different frequencies

Conclusion

A series of uncooled Ti microbolometer was designed and fabricated. The observed experimental data were assessed by electro-thermal circuit simulation. The change in the heater resistance with respect to the current was evaluated based on the electro-thermal simulation and thermal resistances in the structure were extracted. With these values, temperature distribution along the heater line and the responsivity were estimated and compared. The discrepancy in the expected trend from the experimental behaviour was explained by simulated result.

REFERENCES

1. A. Rogalski, *Prog. Quantum Elec.*, **27**, 59 (2003).
2. A. Rogalski and F. Sizov, *Opt. Elec. Rev*. **19**, 346 (2011).
3. M.V.S. Ramakrishna, G. Karunasiri, P. Neuzil, U. Sridhar and W.J. Zeng, *Sens. Actuators A,* **79**, 122 (2000).
4. S. Chen, H. Ma, S. Xiang and X. Yi, *Smart Mater. Struct*., **16**, 696 (2007).
5. V.Y. Zerov, V.G. Malyarov and I.A. Khrebtov, *J. Opt. Technol.*, **78**, 308 (2011).
6. A. Tanaka, S. Matsumoto, N. Tsukamoto, S. Itoh, K. Chiba, T. Endoh, A. Nakazato, K. Okuyama, Y. Kumazawa, M. Hijikawa, H. Gotoh, T. Tanaka and N. Teranishi, *IEEE Trans. Electron Devices*, **43**, 1844 (1996).
7. S. Zhang, Y. Yang, S.M. Sadeghipour and M. Asheghi, Thermal Characterization of the 144 nm GMR Layer using Microfabricated Suspended Structures, Proceedings of ASME Summer Heat Transfer Conference, paper HT 2003-47270, Las Vegas, Nevada, USA, July 21-23 (2003).
8. R. Kato and I. Hatta, *Int J. Thermophys.*, **29**, 2062 (2008).
9. http://en.wikipedia.org/wiki/Titanium